Inorganic Chemistry

Article

pubs.acs.org/IC

QTAIM Analysis of the Bonding in Mo−Mo Bonded Dimolybdenum Complexes

Juan F. Van der Maelen*,[†] and Javier A. Cabeza*,[‡]

[†]Departmento de Química Física and Analítica-CINN, Universidad de Oviedo-CSIC, E-33071 Oviedo, Spain

[‡]Departamento de Química Orgánica and Inorgánica-IUQOEM, Universidad de Oviedo-CSIC, E-33071 Oviedo, Spain

Supporting Information

ABSTRACT: A number of local and integral topological parameters of the electron density of relevant bonding interactions in the binuclear molybdenum complexes $[Mo_2Cl_8]^{4-}$, $[Mo_2(\mu\text{-}CH_3CO_2)_4]$, $[Mo_2(\mu\text{-}CF_3CO_2)_4]$, $[Mo_2(\mu\text{-}CH_3CO_2)_4Br_2]^{2-}$, $[Mo_2(\mu\text{-}CF_3CO_2)_4Br_2]^{2-}$, $[Mo_2(\mu\text{-}CH_3CO_2)_2Cl_4]^{2-}$, $[Mo_2(\mu\text{-}CH_3CO_2)_2(\mu\text{-}Cl)_2Cl_4]^{2-}$, and $[Mo_2(\mu\text{-}Cl)_3Cl_6]^{3-}$ have been calculated and interpreted under the perspective of the quantum theory of atoms in molecules (QTAIM). These data have allowed a comparison between related but different atom−atom interactions, such as different Mo−Mo formal bond orders, ligand-unbridged versus Cl-bridged, CH_3CO_2-bridged, and CF_3CO_2-bridged Mo−Mo interactions, and Mo−$Cl_{terminal}$ and Mo−Cl_{bridge} versus Mo−Br and Mo−O interactions. Calculations carried out using nonrelativistic and relativistic approaches afforded similar results.

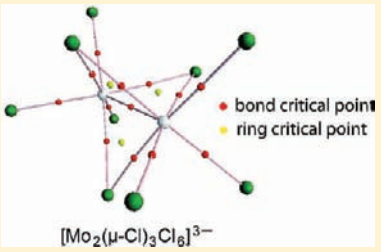

INTRODUCTION

The experimental and theoretical chemistry related to metal−metal multiple bonds was extensively developed after the seminal papers that reported the synthesis and characterization of the anionic complex $[Re_2Cl_8]^{2-}$, which was the first example of a complex having a formal quadruple bond between metal atoms.[1] Most of this research was carried out by F. Albert Cotton's group.[2] In recent times, the appearance on the scene of a compound with a very short Cr−Cr bond distance,[3] corresponding to a formal Cr−Cr quintuple bond,[3,4] has prompted again the search for new compounds having metal−metal bonds with high bond orders.[5,6]

However, in contrast to the abundant theoretical works that have been devoted to study metal−metal bonds under the perspective of the molecular orbital (MO) theory,[2−7] only a few systematic studies on this kind of bonding interactions[8] have hitherto been based on the alternative and complementary approach of the quantum theory of atoms in molecules (QTAIM),[9] which has recently become a powerful tool for studying chemical bonds. QTAIM studies on systems containing light atoms (periods 1−3 of the periodic table) have allowed the establishment of useful links between bonding modes and topological properties (both local and integral) of the electron density and its Laplacian, from both theoretically and experimentally determined electron densities.[10] However, such links cannot be straightforwardly extended to compounds with transition-metal atoms because they display a different and much narrower spectrum of topological indexes.[11] Bonding interactions between transition-metal atoms constitute a particular case, because the QTAIM approach assigns very little (or none at all) electron density to these bonds when they have a low formal bond order (≤1) and, with few exceptions, only finds metal−metal bond paths in these compounds when no bridging ligands are present.[8,12] Additionally, most QTAIM studies on transition-metal complexes have been performed on compounds that have no metal−metal bonds. Therefore, more QTAIM studies on this class of complexes are desirable in order to shed additional light on the relationship between metal−metal bonds and the topology of their associated electron density.

This paper reports the results of a QTAIM study of the bonding in several dimolybdenum complexes with high Mo−Mo formal bond order (≥3). The complexes shown in Figure 1,

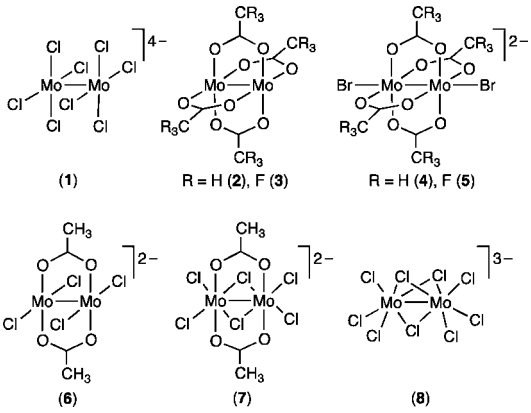

Figure 1. Schematic structures of the dimolybdenum complexes studied in this work.

$[Mo_2Cl_8]^{4-}$ (**1**), $[Mo_2(\mu\text{-}CH_3CO_2)_4]$ (**2**), $[Mo_2(\mu\text{-}CF_3CO_2)_4]$ (**3**), $[Mo_2(\mu\text{-}CH_3CO_2)_4Br_2]^{2-}$ (**4**), $[Mo_2(\mu\text{-}CF_3CO_2)_4Br_2]^{2-}$

Received: April 25, 2012
Published: June 8, 2012

dx.doi.org/10.1021/ic300845g | Inorg. Chem. 2012, 51, 7384−7391

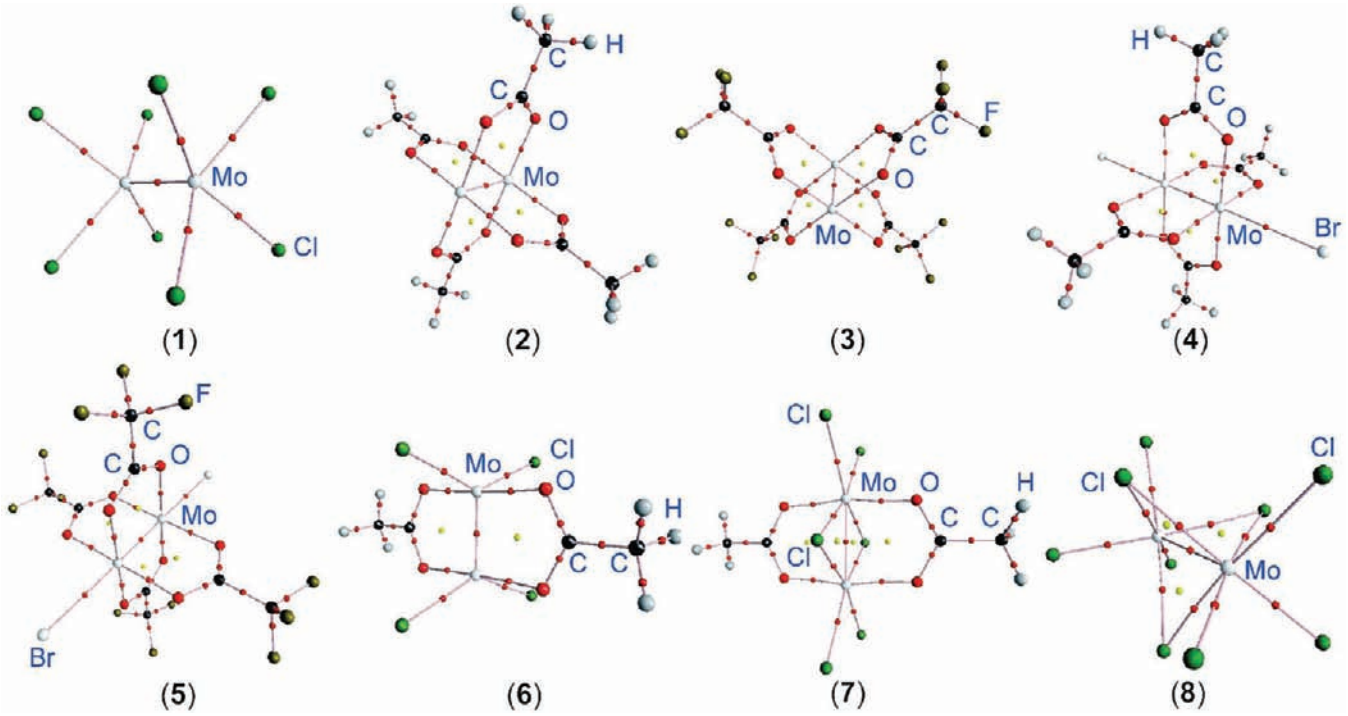

Figure 2. Perspective views of compounds **1**–**8**, showing the bond paths (solid lines) and bond (small red circles) and ring (small yellow circles) critical points. Larger images are provided in the Supporting Information file.

(**5**), $[Mo_2(\mu\text{-}CH_3CO_2)_2Cl_4]^{2-}$ (**6**), $[Mo_2(\mu\text{-}CH_3CO_2)_2(\mu\text{-}Cl)_2Cl_4]^{2-}$ (**7**), and $[Mo_2(\mu\text{-}Cl)_3Cl_6]^{3-}$ (**8**), have been chosen because they allow interesting comparisons between various local and integral topological properties of the electron density of related but different atom–atom interactions. Thus, for a family of complexes having a Mo–Mo formal bond order of 4 (**1**–**6**), we now provide comparisons between Mo–Mo bonds for ligand-unbridged (**1**) versus ligand-bridged complexes (**2**–**6**), acetate-bridged (**2**, **4**) versus trifluoroacetate–bridged complexes (**3**, **5**), tetracarboxylate-bridged complexes without axial ligands (**2**, **3**) versus tetracarboxylate-bridged complexes with two axial ligands (**4**, **5**), and complexes having four carboxylate ligands (**2**, **3**) versus a complex having four terminal Cl ligands and only two bridging carboxylate ligands (**6**). Topological data are also provided for the Mo–Mo bonds of two complexes with a formal bond order of 3 (**7** and **8**) that have different structures, namely, edge-shared bioctahedral (**7**) and face-shared bioctahedral (**8**). In addition, this paper also discusses various topological parameters of the Mo–Cl, Mo–Br, and Mo–O bonds of complexes **1**–**8**. A systematic QTAIM study on binuclear transition-metal complexes of high M–M formal bond order has no precedent in the chemical literature.

Having in mind that it has been previously shown that the use of relativistic Hamiltonians is important to obtain accurate quantitative results from calculations on compounds containing third-row transition-metal atoms,[8b,13] we decided to use both nonrelativistic and relativistic wave functions for our computations on complexes **1**–**8** with the objective of confirming whether or not QTAIM calculations on compounds having a second-row transition-metal, such as molybdenum, are affected by relativistic effects.

■ COMPUTATIONAL METHODS

Density functional theory (DFT) computations with nonrelativistic wave functions were performed with the GAUSSIAN03[14] and GAUSSIAN09[15] program packages using both B3PW91 and B3P86 hybrid functionals[16] (in order to check the accuracy of both methods in our calculations). The structures were optimized using the effective core potential LanL2DZ for the Mo atoms and the all-electron 6-31G(d,p) for the remaining atoms. The previously reported X-ray diffraction structures of $[C_4H_{12}N_2]_2[Mo_2Cl_8]\cdot 4H_2O$,[17] $[Mo_2(\mu\text{-}CH_3CO_2)_4]$,[18] $[Mo_2(\mu\text{-}CF_3CO_2)_4]$,[19] $[C_5H_6N]_2[Mo_2(\mu\text{-}CH_3CO_2)_4Br_2]$,[20] $[NBu_4]_2[Mo_2(\mu\text{-}CF_3CO_2)_4Br_2]$,[21] $[AsPh_4]_2[Mo_2(\mu\text{-}CH_3CO_2)_2Cl_4]\cdot 2CH_3OH$,[22] $[PPh_4]_2[Mo_2(\mu\text{-}CH_3CO_2)_2(\mu\text{-}Cl)_2Cl_4]$,[23] and $[NEt_4]_2[H_3O][Mo_2(\mu\text{-}Cl)_3Cl_3]\cdot 2H_2O$[24] were used as starting points to calculate the optimized geometries of complexes **1**–**8**, respectively. All theoretical models were able to render optimized structures close to the experimental ones, albeit more symmetric (tables of coordinates are available in the Supporting Information file). For instance, all chemically equivalent bonding distances and angles were found to be identical in the optimized structures, although no symmetry constraints were imposed in the geometry optimization processes. The single-point electronic structure calculations at the optimized geometries were performed using B3P86 functional, the large all-electron WTBS ("well-tempered basis set" of Huzinaga and co-workers[25]) for the Mo atoms and the all-electron 6-311++G(3df,3pd) basis set for the remaining atoms.

Computations with relativistic wave functions were performed using the scalar ZORA Hamiltonian, the BP86D3 density functional, and the all-electron TZ2P and QZ4P basis sets for all atoms, as implemented in the ADF2010 program package.[26]

The calculated nonrelativistic (B3P86/WTBS/6-311++G(3df,3pd)) and relativistic (ZORA-BP86D3/TZ2P) ground-state electronic wave functions, which were found to be stable, were then utilized for calculations on the topology of the electron density within the framework of the QTAIM approach. These calculations included both local and integral properties and were carried out with the AIM2000[27] and DGrid[28] programs from GTO- and STO-based wave functions, respectively. The accuracy of the integrated properties was finally set at least at 1.0×10^{-4} (from the Laplacian of the integrated electron density), whereas the accuracy of the local properties was 1.0×10^{-10} (from the gradient of the electron density at the bond critical points). Both all-electron nonrelativistic B3P86/WTBS/6-311++G(3df,3pd) and relativistic ZORA-BP86D3/TZ2P models, applied to the

dx.doi.org/10.1021/ic300845g | Inorg. Chem. 2012, 51, 7384–7391

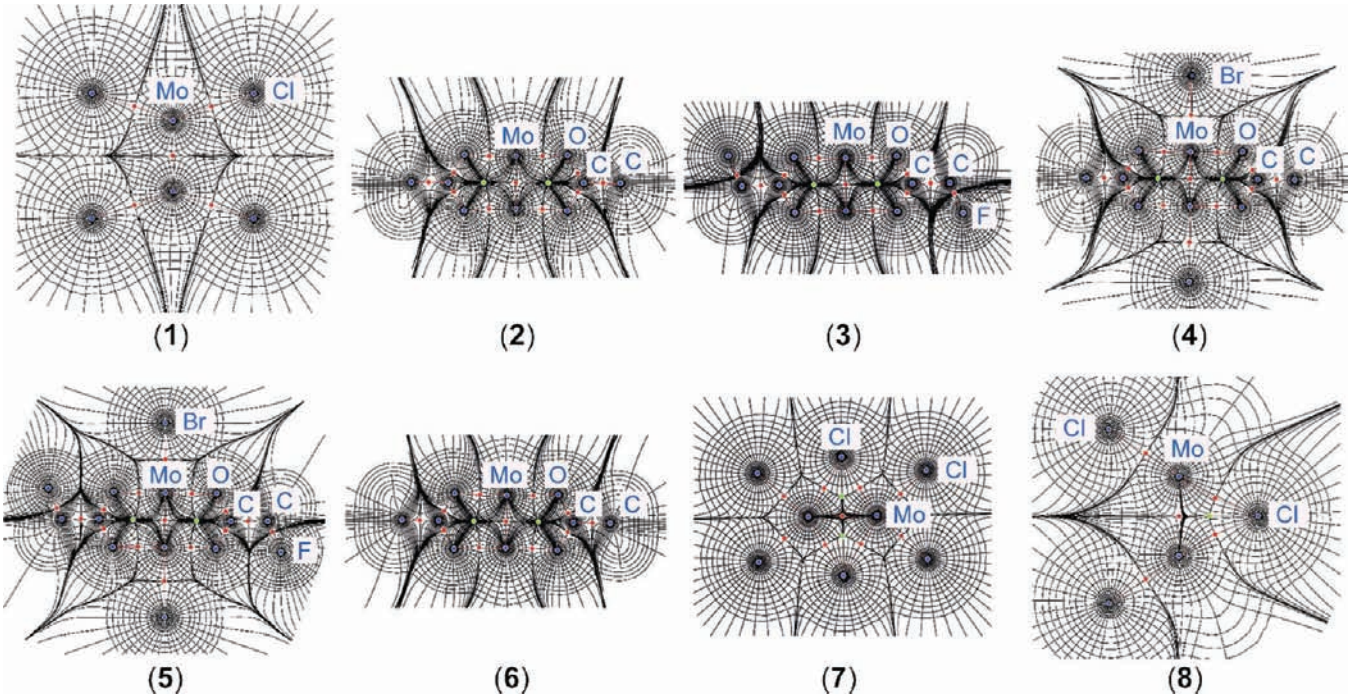

Figure 3. Gradient trajectories mapped on total electron density plots (contour levels at 0.1 e Å^{-3}) in selected planes containing the Mo atoms of **1**−**8**, showing the atomic basins, bps (red lines), bcps (red circles), and rcps (green circles). For symmetry-related atoms, only one atom is labeled. Larger images are provided in the Supporting Information file.

Table 1. Atomic Charges (e) for Selected Atoms of 1−8 [X = $Cl_{terminal}$ (1, 6), Cl_{bridge} (7, 8), O (2, 3), Br (4, 5)]

atom	1	2	3	4	5	6	7	8
				QTAIM				
Mo[a]	1.107	1.344	1.367	1.354	1.359	1.216	1.588	1.480
Mo[b]	1.103	1.354	1.378	1.368	1.375	1.225	1.611	1.501
X[a]	−0.775	−1.144	−1.107	−0.881	−0.814	−0.738	−0.567	−0.603
X[b]	−0.773	−1.144	−1.111	−0.879	−0.817	−0.737	−0.567	−0.606
				Mulliken				
Mo[a]	0.835	1.327	1.362	1.370	1.331	1.158	1.718	1.181
Mo[b]	0.747	1.248	1.303	1.352	1.304	1.048	1.570	1.001
X[a]	−0.708	−0.579	−0.575	−0.914	−0.813	−0.671	−0.433	−0.479
X[b]	−0.686	−0.514	−0.517	−0.921	−0.823	−0.617	−0.380	−0.431
				NBO				
Mo[c]	1.031	1.332	1.358	1.362	1.366	1.156	1.431	1.227
X[c]	−0.758	−0.749	−0.699	−0.922	−0.849	−0.723	−0.500	−0.536

[a]Calculated using the nonrelativistic theoretical model BP86D3/QZ4P. [b]Calculated using the relativistic theoretical model ZORA-BP86D3/QZ4P. [c]Calculated using the nonrelativistic theoretical model B3P86/6-311++G(3df,3pd)/WTBS.

theoretically optimized geometries, were able to find all critical points in all cases and provided similar local or integral topological parameters for each complex.

RESULTS AND DISCUSSION

Topological Properties of the Electron Density. The images shown in Figure 2 were obtained by applying the QTAIM approach to compounds **1**−**8**. They show, along with the atoms corresponding to each complex, the complete set of bond critical points (bcps) and ring critical points (rcps), together with the bond paths (bps) that connect the bonded atoms through their corresponding bcps. Concerning metal−metal interactions, bps for both bridged and unbridged Mo−Mo bonding interactions and their associated bcps were clearly found in the eight complexes, with the bcps located exactly at the geometrical center of each Mo−Mo vector. In regard to metal−ligand interactions, a bcp and a bp were found for each of the two Mo−Br bonding interactions in compounds **4** and **5**, with the bcps located not far from the center of each Mo−Br vector, although slightly closer to the Mo atoms (see Table S9 of the Supporting Information file for the exact A−bcp and bcp−B distances in every A−B bond). Additionally, 8, 4, 8, and 12 bcps and bps, associated to Mo−Cl bonding interactions, were also found for compounds **1**, **6**, **7**, and **8**, respectively; all these bcps are located again slightly closer to Mo atoms than to Cl atoms. Similarly, eight bcps and bps, associated to Mo−O bonding interactions, were found for compounds **2**−**5**, while four of such bcps and bps were located in complexes **6** and **7**. An rcp was obtained for each $Mo_2(\mu\text{-}RCO_2)$ ring of complexes **2**−**7** and for each $Mo_2(\mu\text{-}Cl)$ ring of complexes **7** and **8**.

Figure 3 displays gradient trajectory maps of the total electron density in selected Mo_2X planes of complexes **1**−**8** (X

dx.doi.org/10.1021/ic300845g | Inorg. Chem. 2012, 51, 7384−7391

= Cl for **1**, **7**, and **8**; X = $C_{carboxylate}$ for **2**−**6**), showing the atomic basins of the Mo atoms as well as those of the ligand atoms that are also contained in the chosen planes. The bps, bcps, and rcps located in these planes can also be observed. As expected, the maps corresponding to complexes **2** and **3** are very similar to each other, and the same is true for those corresponding to **4** and **5**. As clearly seen in Figure 3, all bps are straight lines except those corresponding to Mo−Cl_{bridge} interactions (compounds **7** and **8**) that are slightly curved toward the interior of the $Mo_2(\mu$-Cl) triangle.

Integration of the electron density inside each atomic basin rendered the corresponding atomic electric charges. Table 1 compares relativistic and nonrelativistic QTAIM charges with those obtained by other commonly used population analysis methods. While Mulliken and natural bond orbital (NBO) population analyses afforded results rather dependent on the theoretical model used (both method and basis set), the QTAIM approach was very consistent, giving nearly equal values for the charge of each atom regardless of the theoretical model used. In particular, relativistic and nonrelativistic QTAIM charges calculated using the same functional (BP86D3) and basis set (QZ4P) are equal within two significant digits in complexes **1**−**8**, being slightly greater (ca. 0.1 e) than the nonrelativistic NBO charges, while Mulliken charges show significant differences between relativistic and nonrelativistic calculations. As expected by symmetry, both Mo atoms of each complex have identical positive charges, ranging from +1.1 e for the most negatively charged complex (**1**) to +1.6 e for complex **7**. All nonmetal atoms (X) attached to the Mo atoms are negatively charged, ranging from −0.56 e for the bridging Cl atoms of complex **7** to −1.1 e for the O atoms of complex **2**. The O atoms of complexes **4**−**7** have similar negative charges (not included in Table 1).

The electron configurations, obtained from nonrelativistic NBO analyses, of the Mo atoms of complexes **1**−**8** are [core]$5s^{0.21}$ $4d^{4.78}$, [core]$5s^{0.22}$ $4d^{4.47}$, [core]$5s^{0.22}$ $4d^{4.44}$, [core]-$5s^{0.23}$ $4d^{4.43}$, [core]$5s^{0.25}$ $4d^{4.41}$, [core]$5s^{0.22}$ $4d^{4.64}$, [core]$5s^{0.25}$ $4d^{4.33}$, and [core]$5s^{0.27}$ $4d^{4.51}$, respectively, with other noncore orbitals contributing less than 0.1 e.

There are several local (i.e., calculated at the bcp) and integral (i.e., calculated over a whole atomic basin, over an interatomic surface, or along a bond path) topological properties of the electron density that have been successfully used to analyze the bonding in compounds containing transition metals. Among the former, the electron density (ρ_b), the ellipticity (ε_b), the Laplacian of the electron density ($\nabla^2\rho_b$), the kinetic energy density ratio (G_b/ρ_b), and the total energy density ratio (H_b/ρ_b, with $H_b(r) = G_b(r) + V_b(r)$ and $^1/_4\nabla^2\rho_b(r) = 2G_b(r) + V_b(r)$, where $V_b(r)$ is the potential energy density) are by far the most common.[8−12] On the other hand, the delocalization index δ(A−B), which is an integral property, is a useful tool to measure the number of electron pairs delocalized between atoms A and B and can be considered a covalent bond order.[10d,11a,29,30] Values of these topological properties for selected bonds of complexes **1**−**8** are collected in Table 2. These data, obtained using the nonrelativistic B3P86/WTBS/6-311++G(3df,3pd) model, are similar to those obtained using the relativistic ZORA-BP86D3/TZ2P model, which are provided in Table S9 of the Supporting Information file. Therefore, as far as the topological properties studied in this work for complexes **1**−**8** are concerned, the relativistic effects are very small. However, this statement should not be straightforwardly extended to other properties or other second-row transition-metal compounds because the relativistic effects are particular for each molecule. For instance, in a recent study of the Fukui function, no significant relativistic effects were observed for the Au atom of [$AuCl(SMe_2)$] due to the specific environment of this atom in this molecule,[31] while other Au compounds do show strong relativistic effects.

Table 2. Topological Parameters for Selected Bonds of 1−8, Calculated Using the Theoretical Model B3P86/WTBS/6-311++G(3df,3pd) on the Theoretically Optimized Geometries

compd	d^a (Å)	$\rho_b{}^b$ (e Å^{-3})	$\nabla^2\rho_b{}^c$ (e Å^{-5})	$H_b/\rho_b{}^d$ (h e^{-1})	$G_b/\rho_b{}^e$ (h e^{-1})	$\varepsilon_b{}^f$	δ(A−B)^g
			Mo−Mo				
1	2.139	1.159	11.438	−0.094	0.213	0.000	3.314
2	2.131	1.184	12.105	−0.099	0.224	0.001	3.030
3	2.149	1.151	11.377	−0.094	0.212	0.001	3.773
4	2.197	1.083	9.479	−0.086	0.185	0.002	2.907
5	2.243	1.012	8.212	−0.078	0.163	0.002	2.749
6	2.140	1.162	11.564	−0.095	0.215	0.129	3.073
7	2.568	0.556	2.183	−0.029	0.052	0.247	1.860
8	2.334	0.831	4.915	−0.055	0.106	0.004	2.237
			Mo−Cl^h				
1	2.589	0.328	3.759	−0.100	0.901	0.156	0.524
6	2.499	0.402	4.601	−0.145	0.946	0.117	0.586
7	2.526	0.391	3.964	−0.143	0.853	0.121	0.598
8	2.483	0.418	4.460	−0.149	0.896	0.018	0.624
			Mo−Cl^i				
7	2.571	0.349	4.206	−0.121	0.966	0.171	0.516
8	2.616	0.324	4.061	−0.106	0.984	1.180	0.500
			Mo−Br				
4	3.119	0.158	1.372	−0.048	0.657	0.001	0.223
5	2.879	0.248	2.224	−0.114	0.742	0.003	0.336
			Mo−O				
2	2.096	0.587	11.295	−0.099	1.447	0.164	0.526
3	2.091	0.592	11.438	−0.102	1.454	0.155	0.526
4	2.117	0.550	10.708	−0.077	1.440	0.163	0.497
5	2.119	0.548	10.716	−0.075	1.444	0.135	0.494
6	2.113	0.554	10.893	−0.074	1.451	0.190	0.513
7	2.078	0.603	11.923	−0.097	1.481	0.148	0.576

[a]Bond path length. [b]Electron density at the bcp. [c]Laplacian of the electron density at the bcp. [d]Total energy density ratio at the bcp. [e]Kinetic energy density ratio at the bcp. [f]Ellipticity at the bcp. [g]Delocalization index. [h]Average values for terminal Cl ligands. [i]Average values for bridging Cl ligands.

Mo−Mo Interactions. For the Mo−Mo interactions of **1**−**8**, the values given in Table 2 for the electron density at the bcps (between 0.56 e Å^{-3} and 1.18 e Å^{-3}), the positive values of the Laplacian at the bcps (between 2.18 e Å^{-5} and 12.11 e Å^{-5}), the positive but less than unity values of G_b/ρ_b (between 0.05 h e^{-1} and 0.22 h e^{-1}), and the small negative values of H_b/ρ_b (between −0.03 h e^{-1} and −0.10 h e^{-1}) are typical for open-shell metal−metal interactions, intermediate between values for pure covalent and pure ionic bonds between nonmetal atoms. In addition, the bp lengths are very similar to the interatomic distances obtained from X-ray diffraction data[17−24] and also from the theoretically optimized structures (Tables S1−S8 of the Supporting Information). As discussed in the following paragraphs, the topological indexes of compounds **1**−**8** are definitely affected by the structural and compositional features of each complex.

The higher Mo−Mo formal bond order of **1**−**6**, with respect to that of **7** and **8**, results in shorter bp lengths, greater ρ_b,

dx.doi.org/10.1021/ic300845g | Inorg. Chem. 2012, 51, 7384−7391

Table 3. Integrated Electron Density over the Whole Interatomic Surface, $\int_{Mo\cap X}\rho$ (e Å^{-1}), of Selected Bonding Interactions of 1−8, Calculated Using the Theoretical Model B3P86/6-311++G(3df,3pd)/WTBS

Mo−X	1	2	3	4	5	6	7	8
Mo−Mo	3.060	2.473	2.418	2.351	2.254	2.701	1.083	1.544
Mo−Cl$_{terminal}$	1.294					1.268	1.433	1.487
Mo−Cl$_{bridge}$							1.118	1.049
Mo−Br				0.610	0.869			
Mo−O		1.263	1.256	1.252	1.249	1.281	1.417	

much greater $\nabla^2\rho_b$, and greater $|H_b/\rho_b|$ and G_b/ρ_b than those of complexes **7** and **8**.

Within the family of the tetracarboxylate-bridged complexes **2**−**6**, the Mo−Mo bonds of the trifluoroacetate complexes **3** and **5** have longer bp lengths, smaller ρ_b, smaller $\nabla^2\rho_b$, and slightly smaller $|H_b/\rho_b|$ and G_b/ρ_b than those of complexes **2** and **4**, respectively. The presence of axial ligands in tetracarboxylate-bridged complexes is known to result in a small lengthening of the metal−metal bond.[2] Accordingly, the Mo−Mo bonds of the bromide complexes **4** and **5** have slightly longer bp lengths, smaller ρ_b, smaller $\nabla^2\rho_b$, and slightly smaller $|H_b/\rho_b|$ and G_b/ρ_b than those of complexes **2** and **3**, respectively.

The number of acetate bridges in complexes **1**−**6** does not seem to affect the local topological indexes of their Mo−Mo bonds because those of **1** (with no acetate bridges), **2** (with four acetate bridges), and **6** (with two acetate bridges) are very similar. In other words, terminal chlorides and bridging acetates have a similar influence on the local topological indexes of the Mo−Mo bonds.

Despite having Mo−Mo formal bond orders of three, the local topological indexes of the Mo−Mo bonds of complexes **7** and **8** are considerably different. As both have chloride bridges and terminal chloride ligands and as we have herein shown that terminal chlorides and bridging acetates have a similar influence on the topological indexes of the Mo−Mo bonds, the different topological indexes of complexes **7** and **8** should be a consequence of their different structures, edge-sharing bioctahedral and face-sharing bioctahedral, respectively. The presence in both complexes of bridging chloride ligands, which have been previously shown to be very efficient at delocalizing the electron density of the metal−metal bonds they bridge,[8b] and their smaller Mo−Mo formal bond order, in comparison with that of **1**−**6**, may account for the comparatively small values of the local topological indexes of their Mo−Mo bonds (ρ_b, $\nabla^2\rho_b$, $-H_b/\rho_b$, and G_b/ρ_b).

Overall, the local topological indexes of the Mo−Mo bonds of **1**−**8** are in line with those previously reported for $[Mo_2(HNCHNH)_4]$, that is the only binuclear complex having a formal quadruple bond between metal atoms that has been previously studied by QTAIM,[8a] for which ρ_b = 1.118 e Å^{-3} and $\nabla^2\rho_b$ = 12.481 e Å^{-5}, very similar to the values found in the present study for compound **2**. Remarkably, the local topological indexes given in Table 2 for the Mo−Mo bonds of **1**−**8** are considerably different from those previously reported for complexes having metal−metal bonds of lower (mostly single) formal bond order, such as, for instance, the Zn−Zn bond in $[Zn_2(\eta^5\text{-}C_5Me_5)_2]$,[11d] Co−Co bonds in several organometallic compounds,[11e−h] Ru−Ru bonds in $[Ru(CO)_4]_n$,[12e] $[Ru_3(CO)_{12}]$,[12a,g] and $[Ru_3(\mu\text{-}H)_2(\mu_3\text{-}MeImCH)(CO)_9]$,[12f] and Os−Os bonds in $[Os_3(CO)_{12}]$,[8b] among others.[8c] In particular, the values listed in Table 2 for $\nabla^2\rho_b$ are between twice and eight times those found for typical metal−metal single bonds. A similar situation has been found for ρ_b, although the electron density itself is not as sensitive as its Laplacian in order to discriminate between different bond orders. Additionally, the values of H_b/ρ_b and G_b/ρ_b of the Mo−Mo bonds of **1**−**8** are closer to zero than those found for typical metal−metal single bonds. For instance, for $[Zn_2(\eta^5\text{-}C_5Me_5)_2]$,[11d] which contains an unbridged Zn−Zn single bond, values of 0.428 e Å^{-3} and 1.622 e Å^{-5} were found for its ρ_b and its Laplacian at the bcp, respectively, and of −0.361 h e^{-1} and 0.627 h e^{-1} for its H_b/ρ_b and G_b/ρ_b, respectively. Similar values of these indexes have been found for unbridged Co−Co[11e−h] and Ru−Ru[12a,g,f] localized single bonds.

On the other hand, it has been proposed that some integral topological properties are more useful for characterizing metal−metal bonds than the local topological properties.[10d] The delocalization index, δ(A−B), which measures the number of electron pairs delocalized between atoms A and B, is the integral topological property that has been most frequently used.[10d,11a,29,30] The high δ(Mo−Mo) values calculated for **1**−**8** (between 1.9 for complex **7** and 3.8 for complex **3**, see Table 2) clearly indicate that they correspond to Mo−Mo multiple bonds. In comparison, δ(Zn−Zn) = 0.9 for $[Zn_2(\eta^5\text{-}C_5Me_5)_2]$,[11d] δ(Co−Co) = 0.5 for $Co_2(CO)_8$,[11a] and δ(Mo−Mo) = 2.9 for $[Mo_2(HNCHNH)_4]$.[8a]

The integrated electron density over the whole interatomic surface, $\int_{A\cap B}\rho$, which is an integral property too, is also a useful tool to characterize bonding interactions because it is related to the A−B bond strength,[8a,9a,c,d] but unfortunately, it has been seldom applied to metal−metal bonds. The values of $\int_{Mo\cap Mo}\rho$ for **1**−**8** are shown in Table 3. Those of **1**−**6** (in the range 3.06−2.25 e Å^{-1}) not only are clearly higher than those found for the Zn−Zn bond in $[Zn_2(\eta^5\text{-}C_5Me_5)_2]$ (1.25 e Å^{-1}),[11d] the Ru−Ru bond in $[Ru_3(\mu\text{-}H)_2(\mu^3\text{-}MeImCH)(CO)_9]$ (1.36 e Å^{-1}),[12f] the Os−Os bonds in $[Os_3(CO)_{12}]$, $[Os_3(\mu\text{-}H)_2(CO)_{10}]$, $[Os_3(\mu\text{-}H)(\mu\text{-}OH)(CO)_{10}]$, and $[Os_3(\mu\text{-}H)(\mu\text{-}Cl)(CO)_{10}]$ (between 1.44 e Å^{-1} and 1.52 e Å^{-1}),[8b] and the Co−Co bond in $[Co_2(CO)_8]$ (1.56 e Å^{-1}),[11a] but also are noticeably related to the number of bridging ligands, the more bridging ligands the lower the value of $\int_{Mo\cap Mo}\rho$, indicating that some electron density of the Mo−Mo bond is delocalized through their bridging ligands. On the contrary, the $\int_{Mo\cap Mo}\rho$ values listed in Table 3 for complexes **7** and **8** indicate weaker Mo−Mo interactions than in complexes **1**−**6**. This is likely due not only to their lower formal bond order (3 in **7** and **8** versus 4 in **1**−**6**) but also to a more efficient delocalization of the electron density of their Mo−Mo bond through their bridging chloride ligands, which form three-membered $Mo_2(\mu\text{-}Cl)$ rings.[8b]

Mo−Cl, Mo−Br, and Mo−O Interactions. Previous QTAIM studies on complexes containing M−X bonding interactions (M = transition metal, X = halogen) are very scarce, and even rarer are topological studies on di- or polynuclear transition metal complexes containing bridging

dx.doi.org/10.1021/ic300845g | Inorg. Chem. 2012, 51, 7384−7391

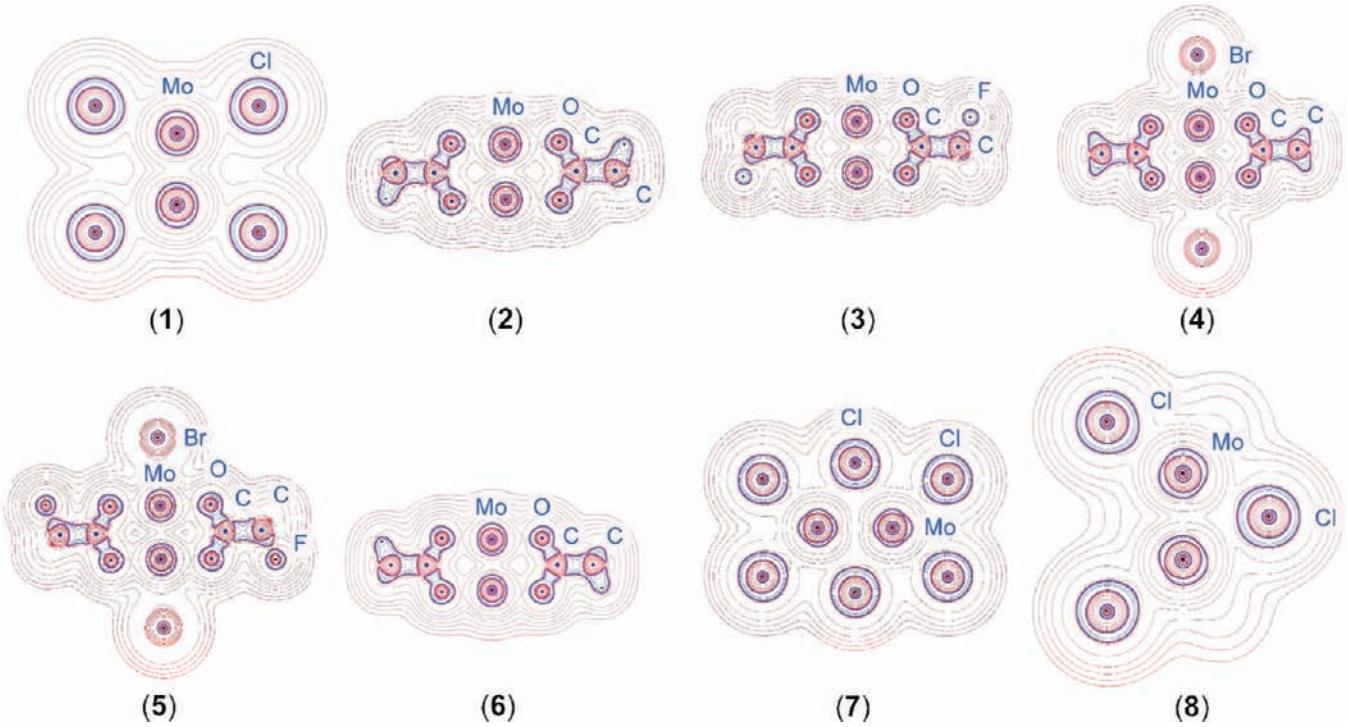

Figure 4. Laplacian of the electron density in relevant planes containing the Mo atoms of **1**−**8** (contour levels at 0.0 and ± (1,2,4,8) × 10^n e Å^{-5}, with *n* ranging from +3 to −3). Blue and red lines represent negative and positive values, respectively. For symmetry-related atoms, only one atom is labeled. Larger images are provided in the Supporting Information file.

halogen ligands, which, to the best of our knowledge are restricted to only one example, namely, the already mentioned triosmium cluster $[Os_3(\mu\text{-H})(\mu\text{-Cl})(CO)_{10}]$.[8b] In this context, we considered it interesting to compare Mo−$Cl_{bridging}$ with Mo−$Cl_{terminal}$ bonds, on the one hand, and the latter with Mo−Br bonds, on the other hand. Although the strength of the Mo−Cl_{bridge} bonds of complexes **7** and **8** is slightly weaker than that of the Mo−$Cl_{terminal}$ bonds, as indicated by their $\int_{Mo\cap Cl}\rho$ (Table 3), the remaining local and integral topological indexes of these bonds are comparable (Table 2). Notably, most topological properties of the Mo−Cl_{bridge} bonds in **7** and **8** are not only very similar to those found for the Os−Cl_{bridge} bonds in $[Os_3(\mu\text{-H})(\mu\text{-Cl})(CO)_{10}]$, but also very much like the M−H_{bridge} (M = Os, Ru) bonds in $[Os_3(\mu\text{-H})_2(CO)_{10}]$,[8b] $[Os_3(\mu\text{-H})(\mu\text{-OH})(CO)_{10}]$,[8b] $[Os_3(\mu\text{-H})(\mu\text{-Cl})(CO)_{10}]$,[8b] and $[Ru_3(\mu\text{-H})_2(\mu_3\text{-MeImCH})(CO)_9]$,[12f] despite the fact that the M−H_{bridge} bond path lengths of the latter are ca. 0.7 Å shorter. As previously commented, these $M_2(\mu\text{-X})$ interactions exhibit some degree of electron delocalization,[8b] notably different from that of the $Co_2(\mu\text{-CO})$ moieties of $[Co_2(\mu\text{-CO})_2(CO)_6]$ and $[Co_4(\mu\text{-CO})_3(CO)_8(PPh_3]$, for which a 3c-4e kind of bonding has been proposed.[11a,12b]

The Mo−$Cl_{terminal}$ interactions of complexes **7** and **8** may be also be analyzed by looking at the Laplacian representations shown in Figure 4, where the valence shell charge depletion (VSCD) of each Mo atom has a pseudocubic shape due to their pseudo-octahedral coordination, slightly deformed due to the off-axis location of their bridging Cl ligands. Valence shell charge concentrations (VSCCs) of both $Cl_{terminal}$ and Cl_{bridge} atoms are distorted toward their bonded Mo atoms, with only one maximum appearing in any of them, as has previously been found for bridging H atoms.[8b,12f] However, while the VSCCs of all $Cl_{terminal}$ atoms are placed exactly opposite to a VSCD of its Mo counterpart, the dispositions of Cl_{bridge} VSCCs are slightly displaced, causing the Mo−Cl_{bridge} bps to be slightly curved inward, as observed in Figure 3. On the other hand, the local topological indexes of the Mo−$Cl_{terminal}$ interactions in compounds **1** and **6** (Table 2) are very similar to those of **7** and **8**, while their integral topological properties are somewhat intermediate between those calculated for the Mo−$Cl_{terminal}$ and Mo−Cl_{bridge} interactions of **7** and **8** (Tables 2 and 3).

It has been experimentally demonstrated that the axial X ligands of $[M_2(\mu\text{-RCO}_2)_4X_2]^{n-}$ complexes are weakly bound to the metal atoms.[2] Consequently, except for their long bp lengths, all local and integral topological properties of the Mo−Br interactions of complexes **4** and **5** are systematically smaller than those of the Mo−$Cl_{terminal}$ and/or Mo−Cl_{bridge} interactions of the remaining complexes. It is also worth noting that, in contrast with that of other atoms, the Laplacian of the electron density around the Br atoms is quite spherical (Figure 4), characterizing the Mo−Br bonds as the closest to pure closed-shell interactions among all bonding types exhibited by complexes **1**−**8**.

Although some topological properties of the Mo−O and Mo−$Cl_{terminal}$ bonds of **1**−**8** are equal within two significant digits, like, for instance, the total energy density ratio at the bcp, the ellipticity at the bcp, the delocalization index (Table 2), and the integrated electron density (Table 3), other properties are clearly different, most notably, the Laplacian of the electron density at the bcp. In fact, the values of $\nabla^2\rho_b$ for the Mo−O bonds in complexes **2**−**7** (in the range 10.7−11.9 e Å^{-5}) are more than twice the values found for the Mo−Cl bonds, being close to those found for the Mo−Mo interactions. Additionally, the calculated charges for O and Cl atoms are also very different, independent of the population analysis method used, with values around −1.1 e for the former and −0.7 e for the latter (Table 1). These differences are also apparent in Figure 4, where the Laplacian of complexes **2**−**6** is depicted in planes

dx.doi.org/10.1021/ic300845g | Inorg. Chem. 2012, 51, 7384−7391

including four Mo−O interactions for each complex. The key-lock mechanism, prototypical of donor−acceptor interactions between a transition-metal atom and a nonmetal atom, is clearly appreciated here. Each O atom points a VSCC directly toward a VSCD of its parent Mo atom, which also exhibits *trans* ligand-induced charge concentrations (LICCs), also called ligand-opposed charge concentrations (LOCCs), in its valence shell. Other examples of this behavior have been found in compounds with carbonyl and alkyl ligands, for which the atomic graph of the metal atom in the Laplacian representation shows vertices (that is, [3, −3] critical points for the Laplacian), that are opposite to a face (that is, a region centered at a [3, +3] critical point for the Laplacian) linked to the ligand.[10b,32] Additionally, a bond charge concentration (BCC), opposite to the Mo−Mo bond and pointing toward each axial coordination site, is also observed in the valence shells of the Mo atoms of the carboxylate-bridged complexes **2**−**6** (Figure 4).

CONCLUDING REMARKS

Theoretical nonrelativistic and relativistic QTAIM topological analyses of the electron density in the binuclear molybdenum complexes $[Mo_2Cl_8]^{4-}$ (**1**), $[Mo_2(\mu\text{-}CH_3CO_2)_4]$ (**2**), $[Mo_2(\mu\text{-}CF_3CO_2)_4]$ (**3**), $[Mo_2(\mu\text{-}CH_3CO_2)_4Br_2]^{2-}$ (**4**), $[Mo_2(\mu\text{-}CF_3CO_2)_4Br_2]^{2-}$ (**5**), $[Mo_2(\mu\text{-}CH_3CO_2)_2Cl_4]^{2-}$ (**6**), $[Mo_2(\mu\text{-}CH_3CO_2)_2(\mu\text{-}Cl)_2Cl_4]^{2-}$ (**7**), and $[Mo_2(\mu\text{-}Cl)_3Cl_6]^{3-}$ (**8**) have allowed a comparison between various local and integral topological properties of related but different atom−atom interactions. The main conclusions of this study follow.

(a) For the studied systems, the data provided by non-relativistic calculations agree, both qualitatively and quantitatively, with the data obtained using relativistic calculations.

(b) A higher Mo−Mo formal bond order (as that of **1**−**6**) results in shorter bp lengths, greater ρ_b, much greater $\nabla^2\rho_b$, and greater $|H_b/\rho_b|$ and G_b/ρ_b (compared with those of **7** and **8**). Concerning integral properties, both the delocalization index, δ(Mo−Mo), and the integrated electron density over the whole interatomic surface, $\int_{Mo\cap Mo}\rho$, are also able to clearly discriminate between different Mo−Mo formal bond orders, with their values for complexes **1**−**6** being markedly greater than those of **7** and **8**.

(c) Within the family of the tetracarboxylate-bridged complexes **2**−**5**, the Mo−Mo bonds in the trifluoroacetate complexes **3** and **5** have longer bp lengths, smaller ρ_b, smaller $\nabla^2\rho_b$, and slightly smaller $|H_b/\rho_b|$ and G_b/ρ_b than those of the acetate complexes **2** and **4**, respectively.

(d) The Mo−Mo bonds of the tetracarboxylate-bridged complexes **4** and **5**, which contain axial bromide ligands, have slightly longer bp lengths, smaller ρ_b, smaller $\nabla^2\rho_b$, and slightly smaller $|H_b/\rho_b|$ and G_b/ρ_b than those of complexes **2** and **3**, respectively, which do not contain axial ligands.

(e) Terminal chlorides and bridging acetates have a similar influence on the local topological indexes of the Mo−Mo bonds of their complexes.

(f) Despite having a Mo−Mo formal bond order of three, the topological indexes of the Mo−Mo bonds of complexes **7** and **8** are considerably different as consequence of their different structures, edge-sharing bioctahedral and face-sharing bioctahedral, respectively.

(g) Bridging chloride ligands are more efficient than bridging carboxylate ligands at delocalizing the electron density of the metal−metal bonds they bridge.

ASSOCIATED CONTENT

Supporting Information

Atomic coordinates for the theoretically optimized geometries of complexes **1**−**8**, topological properties obtained from relativistic calculations, and larger images of the graphical representations provided in Figures 2−4. This material is available free of charge via the Internet at http://pubs.acs.org.

AUTHOR INFORMATION

Corresponding Author

*E-mail: fvu@uniovi.es (J.F.V.), jac@uniovi.es (J.A.C.).

Notes

The authors declare no competing financial interest.

ACKNOWLEDGMENTS

This work has been supported by the Spanish MICINN-FEDER Projects CTQ2010-14933, MAT2010-15094, and CSD2006-00015. We also thank one of the reviewers for his/her helpful comments and for drawing our attention to ref 31.

REFERENCES

(1) (a) Cotton, F. A.; Harris, C. B. *Inorg. Chem.* **1965**, *4*, 30. (b) Cotton, F. A. *Inorg. Chem.* **1965**, *4*, 334.

(2) *Multiple Bonds Between Metal Atoms*, 3rd ed.; Cotton, F. A., Murillo, C. A., Walton, R. A., Eds.; Springer Science and Business Media, Inc.: New York, 2005.

(3) Nguyen, T.; Sutton, A. D.; Brynda, M.; Fettinger, J. C.; Long, G. J.; Power, P. P. *Science* **2005**, *310*, 844.

(4) (a) La Macchia, G.; Li Manni, G.; Todorova, T. K.; Brynda, M.; Aquilante, F.; Roos, B. O.; Gagliardi, L. *Inorg. Chem.* **2010**, *49*, 5216. (b) Brynda, M.; Gagliardi, L.; Roos, B. O. *Chem. Phys. Lett.* **2009**, *471*, 1.

(5) See, for example: (a) Kreisel, K. A.; Yap, G. P. A.; Dmitrenko, O.; Landis, C. R.; Theopold, K. H. *J. Am. Chem. Soc.* **2007**, *129*, 14162. (b) Noor, A.; Wagner, F. R.; Kempe, R. *Angew. Chem., Int. Ed.* **2008**, *47*, 7246. (c) Tsai, Y. C.; Hsu, C. W.; Yu, J. S. K.; Lee, G. H.; Wang, Y.; Kuo, T. S. *Angew. Chem., Int. Ed.* **2008**, *47*, 7250. (d) Hsu, C. W.; Yu, J. S. K.; Yen, C. H.; Lee, G. H.; Wang, Y.; Tsai, Y. C. *Angew. Chem., Int. Ed.* **2008**, *47*, 9933. (e) Horvath, S.; Gorelsky, S. I.; Gambarotta, S.; Korobkov, I. *Angew. Chem., Int. Ed.* **2008**, *47*, 9937.

(6) Takagi, N.; Krapp, A.; Frenking, G. *Inorg. Chem.* **2011**, *50*, 819 and references therein..

(7) See, for example: (a) Hall, M. B. *J. Am. Chem. Soc.* **1980**, *102*, 2104. (b) Kok, R. A.; Hall, M. B. *Inorg. Chem.* **1983**, *22*, 728. (c) Chisholm, M. N.; Davidson, E. R.; Huffmann, J. C.; Quinlan, K. B. *J. Am. Chem. Soc.* **2001**, *123*, 9652. (d) Chisholm, M. N.; Davidson, E. R.; Quinlan, K. B. *J. Am. Chem. Soc.* **2002**, *124*, 15351. (e) Connor, J. A.; Pilcher, G.; Skinner, H. A.; Chisholm, M. H.; Cotton, F. A. *J. Am. Chem. Soc.* **1978**, *100*, 7738. (f) Ziegler, T.; Tschinke, V.; Becke, A. *Polyhedron* **1987**, *6*, 685.

(8) (a) Gatti, C.; Lasi, D. *Faraday Discuss.* **2007**, *135*, 55. (b) Van der Maelen, J. F.; García-Granda, S.; Cabeza, J. A. *Comput. Theor. Chem.* **2011**, *968*, 55. (c) Llusar, R.; Beltrán, A.; Andrés, J.; Fuster, F.; Silvi, B. *J. Phys. Chem. A* **2001**, *105*, 9460. (d) Farrugia, L. J.; Senn, H. M. *J. Phys. Chem. A* **2010**, *114*, 13418. (e) Farrugia, L. J.; Macchi, P. *Struct. Bonding* **2011**, 1.

(9) (a) Bader, R. F. W. *Atoms in Molecules: A Quantum Theory*; Clarendon Press: Oxford, U.K., 1990. (b) Coppens, P. *X-Ray Charge Densities and Chemical Bonding*; International Union of Crystallography and Oxford University Press: Oxford, U.K., 1997. (c) *The Quantum Theory of Atoms in Molecules*; Matta, C. F., Boyd, R. J., Eds.; Wiley-VCH: Weinheim, Germany, 2007. (d) *Modern Charge Density*

Analysis; Gatti, C., Macchi, P., Eds.; Springer: Heidelberg, Germany, 2012.

(10) See, for example: (a) Bader, R. F. W. *J. Phys. Chem. A* **1998**, *102*, 731. (b) Cortés-Guzmán, F.; Bader, R. F. W. *Coord. Chem. Rev.* **2005**, *249*, 633. (c) Koritsanszky, T. S.; Coppens, P. *Chem. Rev.* **2001**, *101*, 1583. (d) Gatti, C. *Z. Kristallogr.* **2005**, *220*, 399. (e) Coppens, P.; Iversen, B. B.; Larsen, F. K. *Coord. Chem. Rev.* **2005**, *249*, 179. (f) Ling, Y.; Zhang, Y. *Annu. Rep. Comput. Chem.* **2010**, *6*, 65. (g) Macchi, P. *Angew. Chem., Int. Ed.* **2009**, *48*, 5793.

(11) (a) Macchi, P.; Sironi, A. *Coord. Chem. Rev.* **2003**, *238*, 383. (b) Farrugia, L. J.; Evans, C.; Tegel, M. *J. Phys. Chem. A* **2006**, *110*, 7952. (c) Farrugia, L. J.; Evans, C.; Lentz, D.; Roemer, M. *J. Am. Chem. Soc.* **2009**, *131*, 1251. (d) Van der Maelen, J. F.; Gutiérrez-Puebla, E.; Monge, A.; García-Granda, S.; Resa, I.; Carmona, E.; Fernández-Díaz, M. T.; McIntyre, G. J.; Pattison, P.; Weber, H.-P. *Acta Crystallogr., Sect. B* **2007**, *63*, 862. (e) Macchi, P.; Proserpio, D. M.; Sironi, A. *J. Am. Chem. Soc.* **1998**, *120*, 13429. (f) Overgaard, J.; Clausen, H. F.; Platts, J. A.; Iversen, B. B. *J. Am. Chem. Soc.* **2008**, *130*, 3834. (g) Macchi, P.; Garlaschelli, L.; Sironi, A. *J. Am. Chem. Soc.* **2002**, *124*, 14173. (h) Bo, C.; Sarasa, J. P.; Poblet, J. M. *J. Phys. Chem.* **1993**, *97*, 6362. (i) Low, A. A.; Kunze, K. L.; MacDougall, P. J.; Hall, M. B. *Inorg. Chem.* **1991**, *30*, 1079. (j) Bianchi, R.; Gervasio, G.; Marabello, D. *Inorg. Chem.* **2000**, *39*, 2360. (k) Van der Maelen, J. F.; Ruiz, J.; García-Granda, S. *J. Theor. Comput. Chem.* **2005**, *4*, 823. (l) Wolstenholme, D. J.; Traboulsee, K. T.; Decken, A.; McGrady, G. S. *Organometallics* **2010**, *29*, 5769. (m) Popov, A. A.; Dunsch, L. *Chem.—Eur. J.* **2009**, *15*, 9707.

(12) (a) Gervasio, G.; Bianchi, R.; Marabello, D. *Chem. Phys. Lett.* **2005**, *407*, 1. (b) Macchi, P.; Garlaschelli, L.; Martinengo, S.; Sironi, A. *J. Am. Chem. Soc.* **1999**, *121*, 10428. (c) Feliz, M.; Llusar, R.; Andrés, J.; Berski, S.; Silvi, B. *New J. Chem.* **2002**, *26*, 844. (d) Bytheway, I.; Griffith, C. S.; Koutsantonis, G. A.; Skelton, B. W.; White, A. H. *Eur. J. Inorg. Chem.* **2007**, 3240. (e) Niskanen, M.; Hirva, P.; Haukka, M. *J. Chem. Theory Comput.* **2009**, *5*, 1084. (f) Cabeza, J. A.; Van der Maelen, J. F.; García-Granda, S. *Organometallics* **2009**, *28*, 3666. (g) Gervasio, G.; Marabello, D.; Bianchi, R.; Forni, A. *J. Phys. Chem. A* **2010**, *114*, 9368. (h) Dinda, S.; Samuelson, A. G. *Chem.—Eur. J.* **2012**, *18*, 3032. (i) Farrugia, L. J.; Evans, C.; Senn, H. M.; Aänninen, M. M.; Sillanpää, R. *Organometallics* **2012**, *31*, 2559.

(13) (a) Eickerling, G.; Mastalerz, R.; Herz, V.; Scherer, W.; Himmel, H.-J.; Reiher, M. *J. Chem. Theory Comput.* **2007**, *3*, 2182. (b) Eickerling, G.; Reiher, M. *J. Chem. Theory Comput.* **2008**, *4*, 286. (c) Hebben, N.; Himmel, H.-J.; Eickerling, G.; Hermann, C.; Reiher, M.; Herz, V.; Presnitz, M.; Scherer, W. *Chem.—Eur. J.* **2007**, *13*, 10078. (d) Reiher, M.; Wolf, A. *Relativistic Quantum Chemistry: The Fundamental Theory of Molecular Science*; Wiley-VCH: Weinheim, Germany, 2009. (e) Fux, S.; Reiher, M. *Struct. Bonding* **2012**, *147*, 99.

(14) Frisch, M. J.; Trucks, G. W.; Schlegel, H. B.; Scuseria, G. E.; Robb, M. A.; Cheeseman, J. R.; Montgomery, J. A., Jr.; Vreven, T.; Kudin, K. N.; Burant, J. C.; Millam, J. M.; Iyengar, S. S.; Tomasi, J.; Barone, V.; Mennucci, B.; Cossi, M.; Scalmani, G.; Rega, N.; Petersson, G. A.; Nakatsuji, H.; Hada, M.; Ehara, M.; Toyota, K.; Fukuda, R.; Hasegawa, J.; Ishida, M.; Nakajima, T.; Honda, Y.; Kitao, O.; Nakai, H.; Klene, M.; Li, X.; Knox, J. E.; Hratchian, H. P.; Cross, J. B.; Adamo, C.; Jaramillo, J.; Gomperts, R.; Stratmann, R. E.; Yazyev, O.; Austin, A. J.; Cammi, R.; Pomelli, C.; Ochterski, J. W.; Ayala, P. Y.; Morokuma, K.; Voth, G. A.; Salvador, P.; Dannenberg, J. J.; Zakrzewski, V. G.; Dapprich, S.; Daniels, A. D.; Strain, M. C.; Farkas, O.; Malick, D. K.; Rabuck, A. D.; Raghavachari, K.; Foresman, J. B.; Ortiz, J. V.; Cui, Q.; Baboul, A. G.; Clifford, S.; Cioslowski, J.; Stefanov, B. B.; Liu, G.; Liashenko, A.; Piskorz, P.; Komaromi, I.; Martin, R. L.; Fox, D. J.; Keith, T.; Al-Laham, M. A.; Peng, C. Y.; Nanayakkara, A.; Challacombe, M.; Gill, P. M. W.; Johnson, B.; Chen, W.; Wong, M. W.; González, C.; Pople, J. A. *GAUSSIAN 03, Revision C.02*; Gaussian, Inc.: Wallingford, CT, 2004.

(15) Frisch, M. J.; Trucks, G. W.; Schlegel, H. B.; Scuseria, G. E.; Robb, M. A.; Cheeseman, J. R.; Scalmani, G; Barone, V.; Mennucci, B.; Petersson, G. A.; Nakatsuji, H.; Caricato, M.; Li, X.; Hratchian, H. P.; Izmaylov, A. F.; Bloino, J.; Zheng, G.; Sonnenberg, J. L.; Hada, M.; Ehara, M.; Toyota, K.; Fukuda, R.; Hasegawa, J.; Ishida, M.; Nakajima, T.; Honda, Y.; Kitao, O.; Nakai, H.; Vreven, T.; Montgomery, J. A., Jr.; Peralta, J. E.; Ogliaro, F.; Bearpark, M.; Heyd, J. J.; Brothers, E.; Kudin, K. N.; Staroverov, V. N.; Keith, T.; Kobayashi, R.; Normand, J.; Raghavachari, K.; Rendell, A.; Burant, J. C.; Iyengar, S. S.; Tomasi, J.; Cossi, M.; Rega, N.; Millam, J. M.; Klene, M.; Knox, J. E.; Cross, J. B.; Bakken, V.; Adamo, C.; Jaramillo, J.; Gomperts, R.; Stratmann, R. E.; Yazyev, O.; Austin, A. J.; Cammi, R.; Pomelli, C.; Ochterski, J. W.; Martin, R. L.; Morokuma, K.; Zakrzewski, V. G.; Voth, G. A.; Salvador, P.; Dannenberg, J. J.; Dapprich, S.; Daniels, A. D.; Farkas, O.; Foresman, J. B.; Ortiz, J. V.; Cioslowski, J.; Fox, D. J. *GAUSSIAN 09, Revision B.01*; Gaussian, Inc.: Wallingford, CT, 2010.

(16) (a) Lee, C.; Yang, W.; Parr, R. G. *Phys. Rev. B* **1988**, *37*, 785. (b) Perdew, J. P. *Phys. Rev. B* **1986**, *33*, 8822. (c) Becke, A. D. *J. Chem. Phys.* **1993**, *98*, 5648.

(17) Leban, I.; Šegedin, P. *Inorg. Chim. Acta* **1984**, *85*, 181.

(18) Hino, K.; Saito, Y.; Bénard, M. *Acta Crystallogr., Sect. B* **1981**, *37*, 2164.

(19) Li, B.; Zhang, H.; Huynh, L.; Shatruk, M.; Dikarev, E. V. *Inorg. Chem.* **2007**, *46*, 9155.

(20) Golic, L.; Leban, I.; Šegedin, P. *Croat. Chem. Acta* **1984**, *57*, 565.

(21) Cotton, F. A.; Fanwick, P. E. *Inorg. Chem.* **1983**, *22*, 1327.

(22) Clegg, W.; Garner, C. D.; Parkes, S.; Walton, I. B. *Inorg. Chem.* **1979**, *18*, 2250.

(23) Cotton, F. A.; Su, J.; Yao, Z. *Inorg. Chim. Acta* **1997**, *266*, 65.

(24) Marsh, R. E. *Acta Crystallogr., Sect. B* **1995**, *51*, 897.

(25) (a) Huzinaga, S.; Miguel, B. *Chem. Phys. Lett.* **1990**, *175*, 289. (b) Huzinaga, S.; Klobukowski, M. *Chem. Phys. Lett.* **1993**, *212*, 260.

(26) Baerends, E. J.; Ziegler, T.; Autschbach, J.; Bashford, D.; Bérces, A.; Bickelhaupt, F. M.; Bo, C.; Boerrigter, P. M.; Cavallo, L.; Chong, D. P.; Deng, L.; Dickson, R. M.; Ellis, D. E.; van Faassen, M.; Fan, L.; Fischer, T. H.; Fonseca-Guerra, C.; Ghysels, A.; Giammona, A.; van Gisbergen, S. J. A.; Götz, A. W.; Groeneveld, J. A.; Gritsenko, O. V.; Grüning, M.; Gusarov, S.; Harris, F. E.; van den Hoek, P.; Jacob, C. R.; Jacobsen, H.; Jensen, L.; Kaminski, J. W.; van Kessel, G.; Kootstra, F.; Kovalenko, A.; Krykunov, M. V.; van Lenthe, E.; McCormack, D. A.; Michalak, A.; Mitoraj, M.; Neugebauer, J.; Nicu, V. P.; Noodleman, L.; Osinga, V. P.; Patchkovskii, S.; Philipsen, P. H. T.; Post, D.; Pye, C. C.; Ravenek, W.; Rodríguez, J. I.; Ros, P.; Schipper, P. R. T.; Schreckenbach, G.; Seldenthuis, J. S.; Seth, M; Snijders, J. G.; Solà, M.; Swart, M.; Swerhone, D.; te Velde, G.; Vernooijs, P.; Versluis, L.; Visscher, L.; Visser, O.; Wang, F.; Wesolowski, T. A.; van Wezenbeek, E. M.; Wiesenekker, G.; Wolff, S. K.; Woo, T. K.; Yakovlev, A. L. *ADF2010, Revision 02*; SCM, Theoretical Chemistry, Vrije Universiteit: Amsterdam, The Netherlands, 2010.

(27) Biegler-König, F.; Schönbohm, J. *J. Comput. Chem.* **2002**, *23*, 1489.

(28) Kohout, M. *DGrid 4.6*; Max Planck Institute for Physical Chemistry of Solids: Dresden, Germany, 2011.

(29) (a) Bertini, L.; Fantucci, G.; De Gioia, L. *Organometallics* **2011**, *39*, 487 and references therein. (b) Matito, E.; Solá, M. *Coord. Chem. Rev.* **2009**, *253*, 647.

(30) Bader, R. F. W; Stephens, M. E. *J. Am. Chem. Soc.* **1975**, *97*, 7391.

(31) Sablon, N.; Mastalerz, R.; De Proft, F.; Geerlings, P.; Reiher, M. *Theor. Chem. Acc.* **2010**, *127*, 195.

(32) (a) Bytheway, I.; Gillespie, R. J.; Tang, T.-H.; Bader, R. F. W. *Inorg. Chem.* **1995**, *34*, 2407. (b) Scherer, W; Sirsch, P.; Shorokhov, D.; Tafipolsky, M.; McGrady, G. S.; Gullo, E. *Chem.—Eur. J.* **2003**, *9*, 6057.